Left ventricular interaction with arterial load studied in isolated canine ventricle

KENJI SUNAGAWA, W. LOWELL MAUGHAN, DANIEL BURKHOFF, AND KIICHI SAGAWA
Departments of Biomedical Engineering and Medicine, The Johns Hopkins Medical Institutions, Baltimore, Maryland 21205

SUNAGAWA, KENJI, W. LOWELL MAUGHAN, DANIEL BURKHOFF, AND KIICHI SAGAWA. *Left ventricular interaction with arterial load studied in isolated canine ventricle.* Am. J. Physiol. 245 (Heart Circ. Physiol. 14): H773–H780, 1983.—We developed a framework of analysis to predict the stroke volume (SV) resulting from the complex mechanical interaction between the ventricle and its arterial system. In this analysis, we characterized both the left ventricle and the arterial system by their end systolic pressure (P_s)-SV relationships and predicted SV from the intersection of the two relationship lines. The final output of the analysis was a formula that gives the SV for a given preload as a function of the ventricular properties (E_{es}, V_0, and ejection time) and the arterial impedance properties (modeled in terms of a 3-element Windkessel). To test the validity of this framework for analyzing the ventriculoarterial interaction, we first determined the ventricular properties under a specific set of control arterial impedance conditions. With the ventricular properties thus obtained, we used the analytical formula to predict SVs under various combinations of noncontrol arterial impedance conditions and four preloads. The predicted SVs were compared with those measured while actually imposing the identical set of arterial impedance conditions and preload in eight isolated canine ventricles. The predicted SV was highly correlated ($P < 0.0001$) with the measured one in all ventricles. The average correlation coefficient was 0.985 ± 0.004 (SE), the slope 1.00 ± 0.04, and the *y*-axis intercept 1.0 ± 0.2 ml, indicating the accuracy of the prediction. We conclude that the representations of ventricle and arterial system by their P_s-SV relationships are useful in understanding how these two systems determine SV when they are coupled and interact.

ventriculoarterial coupling; end-systolic pressure vs. stroke volume relationship; ventricular model; arterial model

GUYTON AND HIS ASSOCIATES (1, 2, 4) in the 1950s opened the hydraulic loop of the circulatory system at the junction of the vena cava and the right atrium. They graphically showed that the changes in cardiac output in the closed circulatory system could be explained as the shift of intersection (i.e., the equilibrium point) between the cardiac output curve and venous return curve, both of which were functions of mean right atrial pressure. This approach has been very useful in understanding the roles of various factors that determine cardiac output. However, the specific roles of the right vs. left sides of the heart and of the systemic vs. pulmonary vascular bed in determining the cardiac output were obscure in their analysis. Subsequently Herndon and Sagawa (3) divided the circulatory loop in two sections, the heart-lung section and the systemic vascular bed section, and gave an empirical description of the cardiac output through the heart-lung section as a function of mean right atrial pressure and mean systemic arterial pressure. Although this analysis showed the influence of systemic arterial pressure on cardiac output, it was still unclear how individual components of the heart-lung section, such as the cardiac chambers and the pulmonary vascular system parameters, interact with each other to determine the cardiac output.

Piene (5) and Piene and Sund (6) recently analyzed the coupling of the right ventricle with the pulmonary arterial system. Using an iterative algorithm, they computed instantaneous right ventricular pressure, pulmonary arterial pressure, and flow, representing the mechanical properties of the right ventricle with its instantaneous pressure-volume (P-V) relationship and those of the pulmonary arterial system by its hydraulic impedance. The instantaneous flow and pressures thus computed agreed with experimental data obtained in an isolated feline right heart preparation. This suggested that the P-V relationship and the hydraulic impedance used could adequately represent ventricular and arterial system mechanical properties, respectively, for the purpose of describing the ventriculoarterial coupling. Since this analysis was numerical, it did not clarify the interrelationship among individual determinants of cardiac output nor did it add any conceptual insight into the mechanism by which each of the component parameters affect the interaction. If, on the other hand, one can analytically derive an equation that relates cardiac output or stroke volume to the properties of the ventricle and of the vascular system, this would be more helpful in understanding the ventriculoarterial interaction.

The purpose of the present investigation was to examine, in isolated canine ventricles, the accuracy of a model that analytically describes the stroke volume resulting from the complex ventriculoarterial coupling for a given set of ventricular and arterial system parameters.

THEORETICAL CONSIDERATIONS

A series of experiments on canine ventricles in our (10, 12) and other laboratories (16–18) indicated that the end-systolic pressure-volume relationship (ESPVR) was approximately linear over a physiological range and,

0363-6135/83 $1.50 Copyright © 1983 the American Physiological Society

while its slope (E_{es}) varied greatly in response to changes in contractility, the ESPVR was insensitive to changes in loading conditions (Fig. 1). Thus Suga and co-workers (10, 12) described the relation of the left ventricular end-systolic pressure (P_{es}) to stroke volume (SV) as

$$P_{es} = E_{es}(V_{ed} - SV - V_0) \quad (1)$$

where V_{ed} is the end-diastolic volume and V_0 the volume axis intercept of the ESPVR. Therefore, for a given V_{ed}, P_{es} varies inversely with SV in a linear way (left middle panel in Fig. 2).

If we also express the arterial system properties by a P_{es}-SV relationship (right middle panel of Fig. 2), then the SV that results when the ventricle is actually coupled with the arterial system is given as the intersection between the ventricular P_{es}-SV relationship and the arterial P_{es}-SV relationship (bottom panel of Fig. 2). Therefore the question is whether we can analytically describe the P_{es}-SV relationship of the arterial system. If the arterial system properties are approximated by a three-element Windkessel model consisting of characteristic impedance (R_c), peripheral resistance (R), and arterial compliance (C) as shown in Fig. 3*A*, arterial flow (AF) averaged over the duration (T) of one cardiac cycle is obtained as

$$\overline{AF} = \frac{\overline{AP}}{R_c + R} \quad (2)$$

where $\overline{AP}$ is arterial pressure averaged over one cardiac cycle. Since mean arterial flow equals SV/T, and mean arterial pressure equals the total area (A_T) under the arterial pressure curve (Fig. 3*B*) over one cardiac cycle divided by T, *Eq. 2* can be rewritten as

$$\frac{SV}{T} = \frac{A_T/T}{R_c + R} \quad (3)$$

Therefore, stroke volume can be related to A_T and $R_c + R$ as

$$SV = A_T/(R_c + R) \quad (4)$$

The end-systolic pressure in *Eq. 1* is in general slightly different from the end-ejection pressure (7). However, if we disregard this small difference and denote both the end-ejection pressure and the end-systolic pressure by P_s, the diastolic pressure area A_d in Fig. 3*B* can be approximated by

$$A_d^* = P_s\tau[1 - \exp(-t_d/\tau)] \quad (5)$$

where t_d is the duration of "arterial diastole" and τ is the time constant of the diastolic arterial pressure decay, which is equal to the product of the arterial resistance (R) and compliance (C). The asterisk indicates that *Eq. 5* is an approximation of the true A_d. Approximating the systolic pressure area (A_s) by the rectangle shown in Fig. 3 yields an approximation of A_s as

$$A_s^* = P_s t_s \quad (6)$$

where t_s is the ejection time. Adding *Eqs. 5* and *6* yields an approximation of A_T (= $A_s + A_d$) as

$$A_T^* = P_s\{t_s + \tau[1 - \exp(-t_d/\tau)]\} \quad (7)$$

The asterisk will be dropped hereafter. Substituting the approximate A_T described by *Eq. 7* into the true A_T in *Eq. 4* yields an approximated P_s-SV relationship of the arterial system

$$P_s = \frac{R_c + R}{t_s + \tau[1 - \exp(-t_d/\tau)]} SV \quad (8)$$

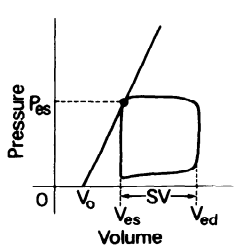

FIG. 1. Schematic diagram of end-systolic pressure-volume (P_{es}-V_{es}) relationship. SV, stroke volume; V_{ed}, end-diastolic volume; V_{es}, end-systolic volume; V_0, volume axis intercept of P_{es}-SV relationship.

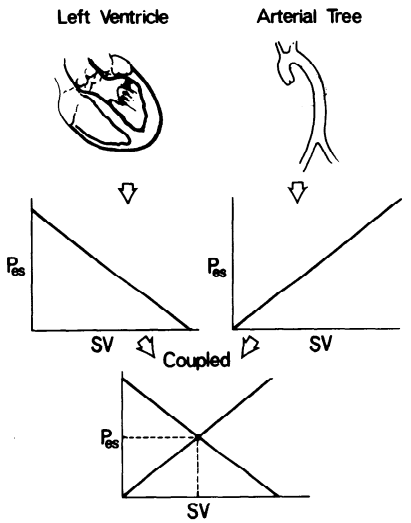

FIG. 2. Representation of the proposed approach of coupling the ventricle with the arterial load. Mechanical characteristics of left ventricle are expressed by an end-systolic pressure (P_{es}) vs. stroke volume (SV) relationship (*left middle panel*). Similarly, mechanical characteristics of arterial system are expressed by P_{es}-SV relationship (*right middle panel*). Equilibrium SV when the ventricle is coupled with the arterial system is obtained as an intersection between these 2 P_{es}-SV relationship lines (*bottom panel*).

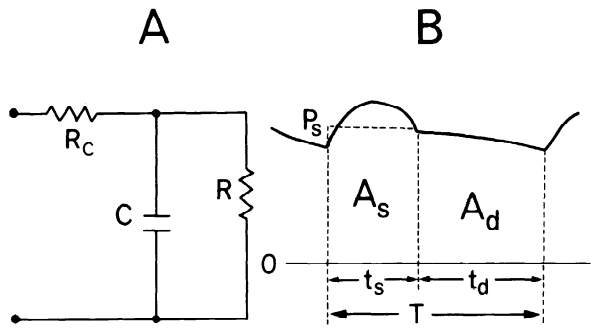

FIG. 3. *A*: electrical analog of 3-element Windkessel arterial model. R_c, characteristic impedance; C, arterial compliance; R, arterial resistance. *B*: schematic diagram of arterial pressure curve. Area under pressure curve during systole (A_s) is approximated by the product of P_s and ejection time (t_s). Area under pressure curve during arterial diastole (A_d) is obtained using *Eq. 3*. t_d, Diastolic interval; T, 1 cardiac period.

The equation states that P_s increases linearly with SV (as shown in the middle right panel of Fig. 2) if the vascular parameters (R_c, R, and C) and t_s and t_d remain constant. If we denote the slope of the P_s-SV relationship by E_a (effective arterial elastance), i.e., $E_a = (R_c + R)/\{t_s + \tau[1 - \exp(-t_d/\tau)]\}$, *Eq. 8* becomes

$$P_s = E_a\ SV \qquad (9)$$

Since the analytical relationship of the P_s to SV in the left ventricle is described by *Eq. 1* and that in the arterial system by *Eq. 9*, the equilibrium SV in the ventriculoarterial-coupled system can be obtained by simultaneously solving these two equations as

$$SV = \frac{V_{ed} - V_0}{1 + E_a/E_{es}} \qquad (10)$$

The validity of this approximate relation was tested in isolated canine left ventricles that ejected into a simulated arterial impedance system.

METHODS

Preparation. The surgical preparation of an isolated canine ventricle has been described elsewhere (9, 11). Briefly, a pair of mongrel dogs weighing 20–22 kg was used in each experiment under anesthesia with pentobarbital sodium (30 mg/kg iv). The chest of the heart donor was opened under artificial ventilation. The subclavian artery and right atrium were cannulated and connected to the femoral arteries and veins, respectively, of a support dog. After ligation of the azygos vein, superior and inferior venae cavae, brachiocephalic artery, descending aorta, and pulmonary hili, the heart was removed from the chest. The pericardium was removed, and the left and right ventricles were vented. The chordae tendinae were cut. A thin balloon mounted on a plastic adaptor was fitted into the left ventricle, and the adaptor was sewn into the mitral valve annulus. The balloon adaptor was then connected to a ventricular volume control servo pump system (11, 14). A constant volume of tap water filled the pump and balloon. Therefore, absolute volume changes in the balloon were precisely controlled and measured by the volume servo pump. A disk oxygenator (Pemco model 7109) was placed in parallel with the support dog so that oxygenated blood could be received either from the support dog or from the oxygenator as desired. Coronary arterial pressure was measured by a catheter placed via the brachiocephalic trunk in the aortic root. A servo controlled perfusion pump (Harvard Apparatus model 1215) maintained mean coronary arterial pressure at 100 mmHg. Coronary arterial blood temperature was maintained approximately at 37°C with a heat exchanger. The left ventricular pressure was measured in the balloon with a catheter tip micromanometer (Millar model PC-380). Ventricular P-V loops were monitored on-line on an *X-Y* storage oscilloscope and photographed by a Polaroid camera. Ventricular pressure, volume, coronary arterial pressure, and arterial pressure of the support dog were recorded on an eight-channel chart recorder.

Impedance loading system. A schematic diagram of the impedance loading system (13) is shown in Fig. 4. We used a three-element Windkessel model (Fig. 3*A*) as the afterload system (Ejection in Fig. 4) and a simple DC pressure source coupled with a filling resistance in series as the preload system (Filling in Fig. 4). We programmed the simulated afterload and preload system models on an analog computer to calculate in real-time the instantaneous flow out of or into the ventricle that should occur

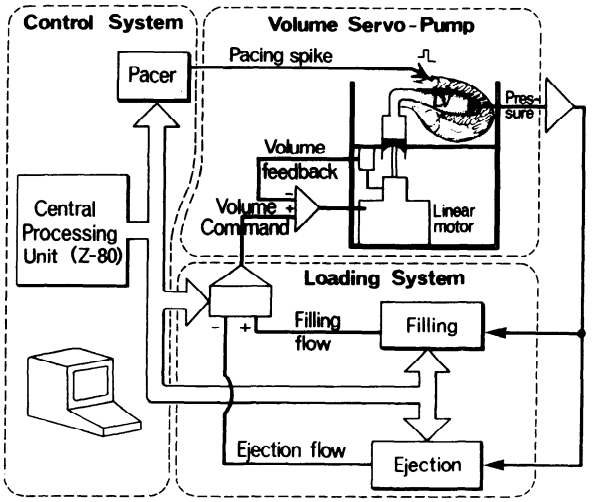

FIG. 4. Schematic diagram of the impedance loading system (14). Volume servo control pump, which consists of a linear motor and a piston pump, enables us to control and measure instantaneous ventricular volume precisely. Excised left ventricle is attached to this volume servo pump. Loading system computes instantaneous flow into or out of the ventricle in real-time in response to given instantaneous ventricular pressure. Computed flow is integrated and integral is used as command signal to the volume servo pump. Control system consists of a digital computer that lets experimenter set the parameter values in the loading system.

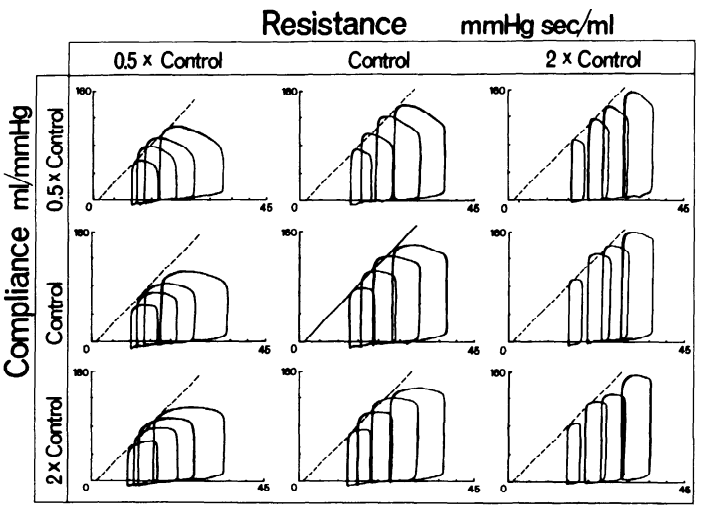

FIG. 5. Example of a typical set of data. Multiple pressure-volume (P-V) loops were obtained by varying resistance and compliance from 50 to 200% of their control values at 4 different end-diastolic volumes under each combination of the resistance and compliance values. Characteristic impedance was kept at control. A *solid line* in center panel indicates end-systolic P-V relationship line under a control loading condition. *Dashed lines* in other panel indicate transcribed end-systolic P-V relationship line from control. Although there were some variations in the end-systolic P-V relationship under a wide variety of loading conditions, they were rather small quantitatively.

in response to the actual instantaneous ventricular pressure of the isolated heart. This calculated instantaneous flow was integrated, and the integral was used as the command signal to the volume servo pump. With this loading system, the ejection pattern and stroke volume were dependent on the interaction between the real ventricle and the afterload system parameters (R_c, R, and C) set in the analog computer model by the experimenter through a digital computer (Radio Shack TRS-80) based on Z-80 (Zilog).

Protocol. We first obtained P-V loops under control afterload condition at four different end-diastolic volumes as shown in the central "control" panel of Fig. 5. Control values chosen for the characteristic impedance, resistance, and compliance of the arterial model were 0.2 mmHg·s·ml^{-1}, 3.0 mmHg·s·ml^{-1}, and 0.4 ml/mmHg, respectively. We then changed the values of the afterload resistance and/or compliance from 50 to 200% of their control values in a random sequence and obtained the left ventricular P-V loops at four different end-diastolic

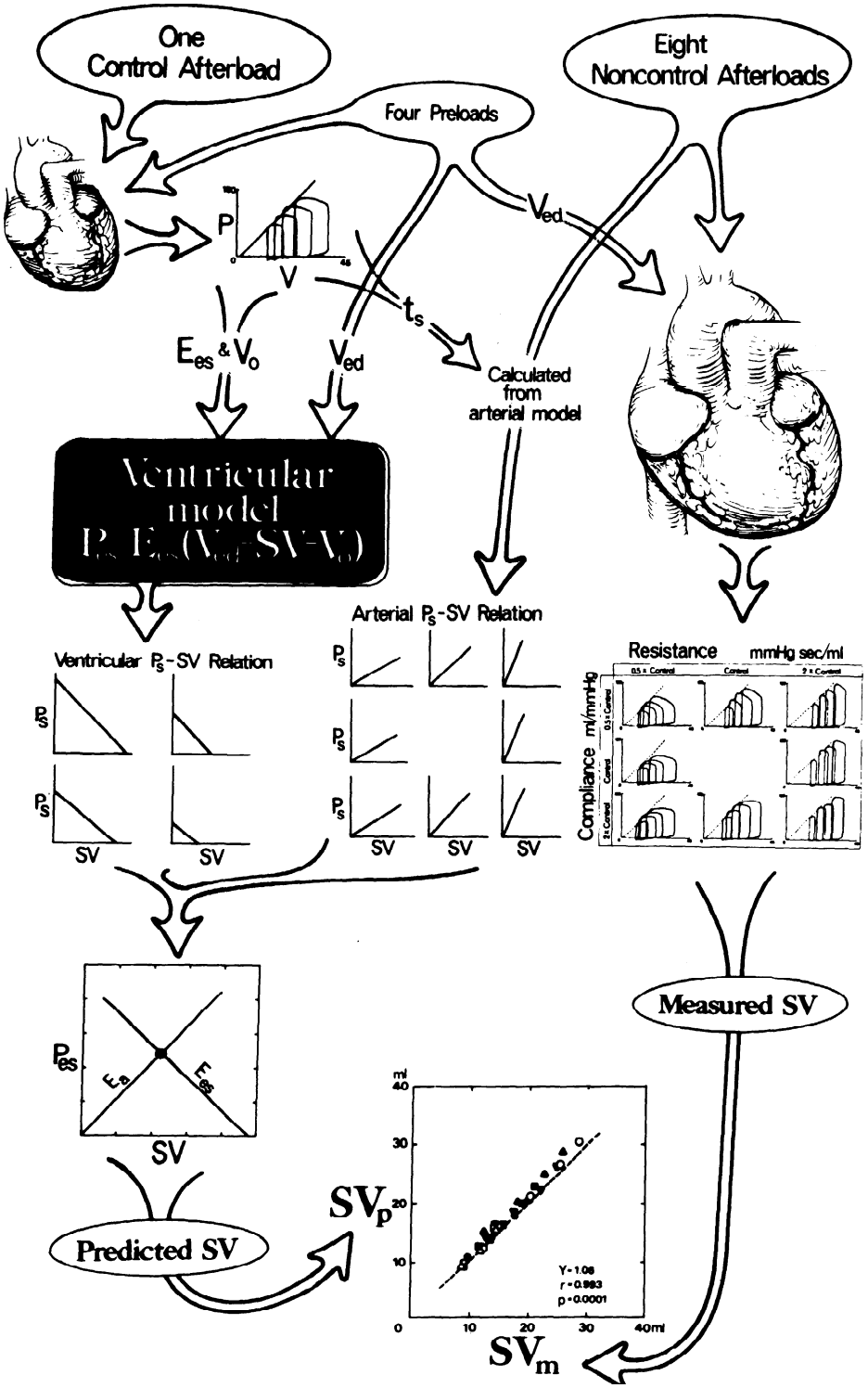

FIG. 6. Flow chart of validation procedure of proposed framework of ventriculoarterial coupling (see text).

volumes under each of eight different afterload conditions (Fig. 5). Finally, we obtained the P-V loops under the control afterload condition again. If the E_{es} value obtained from these loops changed more than 10% compared with that from the first control loops, we discarded the data set. Heart rate was kept constant in each ventricle (127 ± 9 beats/min) by pacing from either the right or left atrium.

Data analysis. Presented in Fig. 6 is a flow chart that explains how we tested the validity of the proposed framework of analysis of ventriculoarterial interaction. The most important hypothesis is that the end-systolic pressure-volume relationship is independent of a specific arterial impedance condition under which the relationship was determined. As shown in the top left corner of the chart in Fig. 6, the control afterload and four preloads were imposed on a given heart. The heart generated four P-V loops from which the values for E_{es}, V_0, and t_s were determined. This set of values was assumed to be valid for other end-systolic P-V relations under noncontrol afterloads. With this hypothesis, the E_{es} and V_0 values were plugged in the ventricular model shown in the midleft part of the chart. Imposing the same four preloads on the ventricular model, we obtained a set of four ventricular P_s-SV relation lines that were combined with eight arterial P_s-SV relation lines by *Eq. 10* to predict stroke volumes under the eight afterloads.

As shown in the center part of the chart, the arterial P_s-SV relation lines (i.e., E_a value) were calculated by feeding the t_s value from the given heart (determined under the control afterloading condition) and eight afterloads (shown in upper right corner), which have values of R, R_c, and C different from the control set, into *Eq. 8*. Remember that a simplifying assumption was used in deriving *Eq. 8*. Therefore, the validity of this assumption was also tested when the predicted and measured stroke volumes were compared as described later. A total of 32 stroke volumes was calculated from *Eq. 10* for a given heart.

The same heart, redrawn in the right upper corner of the chart, had the same four preloads and eight noncontrol afterloads imposed on it, and a total of 32 stroke volumes was measured. These measured stroke volumes were plotted against the predicted stroke volumes calculated under the identical preload and afterload conditions to generate a scatter diagram shown at the bottom of the chart. Since we studied eight left ventricles, eight such scatter diagrams were obtained (see Figs. 8 and 9). We applied linear regression analysis of the predicted stroke volume on actual stroke volume to judge the accuracy of the prediction.

RESULTS

We obtained the complete data sets (Fig. 5) under nine afterloading conditions in eight isolated canine ventricles. The mean E_{es} value from all the data in all ventricles was 5.4 ± 1.0 mmHg/ml (SE), the mean V_0 was 8.2 ± 2.3 ml, and the mean ejection time was 160 ± 12 ms. Figure 7 shows a representative example of the arterial P_s-SV relationship. Figure 7*A* indicates the P_s-SV relationship under arterial resistance values of 50, 100, and 200% of control while the compliance was maintained at control. The plotted points represent measured P_s-SV relationship data, whereas the solid lines indicate the P_s-SV relationship generated by *Eq. 8* incorporating the specific vascular parameter values while keeping t_s value at control. First, it is clear that the slope of the measured arterial P_s-SV relationship is highly dependent on the arterial resistance. The slope increased with increases in arterial resistance. Second, the predicted P_s-SV relationships by *Eq. 8* were very close to those actually measured, indicating that *Eq. 8* is a good approximation of the P_s-SV relation in the arterial loading system. Figure 7*B* shows the arterial P_s-SV relationship under arterial compliance values of 50, 100, and 200% of control while the resistance was fixed at control value. The slope of the measured arterial P_s-SV relationship decreased with increases in the arterial compliance. However, for comparable changes in the values of resistance and compliance, the slope changes with resistance (Fig. 7*A*) were far greater than those with compliance (Fig. 7*B*). Again the predicted arterial P_s-SV relationship lines with these compliance values are very close to those actually measured.

Figure 8 shows an example of the relationship between the predicted and measured stroke volumes under various values of arterial resistance, compliance and end-diastolic volume. All the data in this plot were obtained from a single ventricle. Each different symbol represents data with different combinations of arterial resistance and compliance. The correlation coefficient in this example was 0.993 ($P < 0.0001$), and the linear regression equation was $Y = 1.06X + 0.3$. The slope of the regression line was close to unity with a very small y-axis intercept indicating the accuracy of the prediction. Figure 9 shows the relationship between the predicted vs. measured SVs in the seven other ventricles. The average correlation coefficient was 0.985 ± 0.004 (SE), the slope 1.00 ± 0.04, and the y-axis intercept 1.0 ± 0.2 ml. Thus our model was able to predict the stroke volume reasonably well in all the left ventricles studied.

DISCUSSION

Coupling model framework. We have shown that the proposed model that couples the left ventricle to the

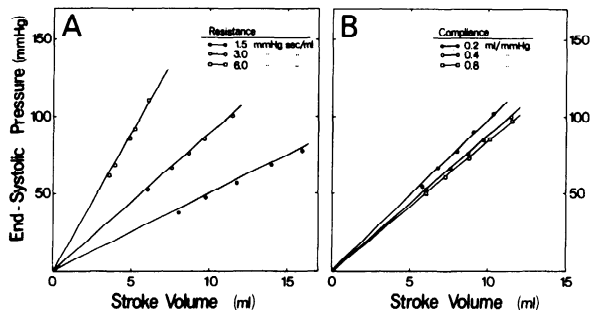

FIG. 7. End-systolic pressure vs. stroke volume relationship of the arterial system. *Solid lines* represent relationships predicted by *Eq. 7*. *Plotted symbols* represent actual data obtained from an experiment. *A*: slope of the line markedly increased with increases in arterial resistance. *B*: slope of the relationship line only mildly increased with decreases in arterial compliance.

arterial system can accurately predict the stroke volume. This coupling was made possible by representing the functions of both the ventricle and the arterial system in terms of their P_s-SV relationships (Fig. 10*A*). Since the slopes of both these P_s-SV relationships have the dimension of volume elastance (mmHg/ml), we are treating the arterial system as if it is an elastic chamber that has the volume elastance E_a just as we treat the ventricle as an elastic chamber with the end-systolic elastance E_{es}. With such representations, our prediction of the equilibrium stroke volume when the ventricle is coupled to the arterial system is similar to asking: How much volume will be transferred if one couples an elastic chamber (left ventricle) with a known volume elastance, dead volume, and initial volume, to a second elastic chamber (arterial system) with a known volume elastance (Fig. 10*B*)? Obviously, the distribution of the volume between the two chambers will be determined by the ratio of their volume elastance values. The slope of the arterial P_s-SV relationship represents neither the physical elastance nor compliance of arterial system but an "effective" arterial elastance. As shown in Fig. 7, the effective arterial elast-

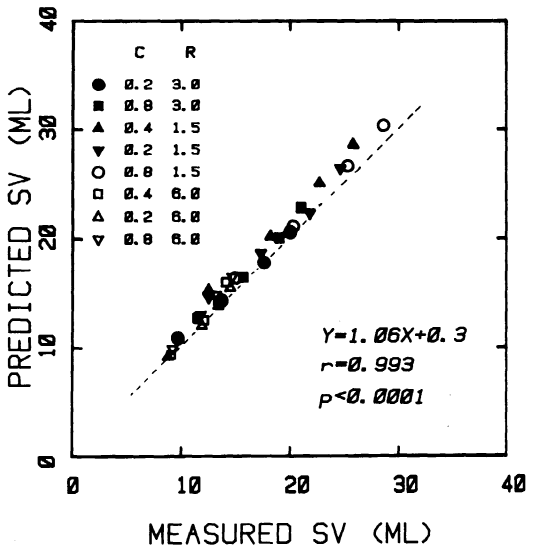

FIG. 8. Representative example of predicted and measured stroke volume (SV) relationship obtained in one ventricle. *C*, compliance (ml/mmHg); *R*, resistance (mmHg·s·ml^{-1}). *Different symbols* represent different loading conditions. Despite a wide range of loading conditions, data were tightly distributed along the identity line (*dashed line*), indicating accuracy of prediction.

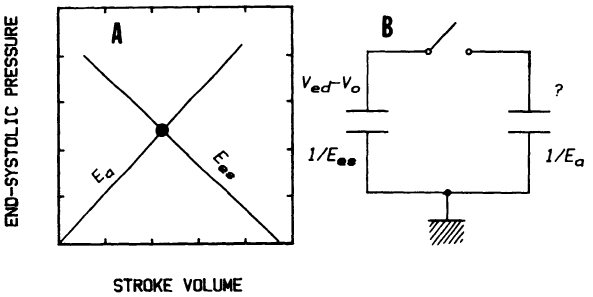

FIG. 10. *A*: graphical determination of equilibrium stroke volume when ventricle with a volume elastance E_{es} is coupled to the arterial system with a volume elastance E_a. Stroke volume is obtained as the abscissa of the intersection between these 2 lines. *B*: physical meaning of the proposed ventriculoarterial coupling model. Both ventricle and arterial system are considered as elastic chambers with known volume elastances (E_{es} and E_a, respectively). Stroke volume is determined as the amount of fluid transferred from the ventricle to the arterial system when the two are connected.

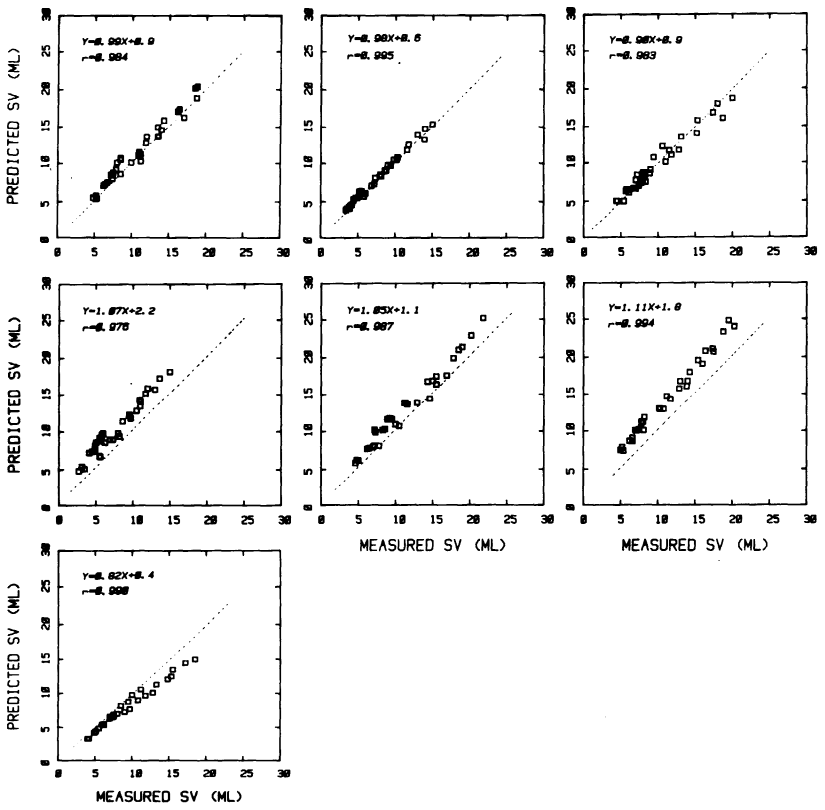

FIG. 9. Summary of the predicted vs. measured stroke volume (SV) correlationship from the other 7 ventricles.

ance changes more with changes in physical arterial resistance than with changes in physical arterial compliance. The greater effect of resistance contributed to the physiological observation that, within the scope of change from 50 to 200% of their control, the arterial resistance was far more important than the arterial compliance in determining SV.

The following examples may illustrate how this simplified approach to coupling enables us to quickly evaluate the specific contributions of ventricular end-systolic properties and the arterial system parameters in determining SV. If V_{ed} is increased, the ventricular P_s-SV relationship will shift rightward (thick arrow, Fig. 11*A*) without a change in the slope (*Eq. 1*) because E_{es} is insensitive to changes in preload. The abscissa of the intersection between the ventricular and arterial P_s-SV relation lines represents the equilibrium SV. With an increase in V_{ed}, the ventricular P_s-SV relation line shifts rightward, and the SV increases from control equilibrium value (open circle) to a new equilibrium value (closed circle). If the contractility of the ventricle is augmented (i.e., if E_{es} increases), the slope of the ventricular P_s-SV relationship will increase without changes in the SV-axis intercept (thick arrow, Fig. 11*B*) as long as the V_{ed} is held constant (*Eq. 1*). If there is no change in the arterial P_s-SV relationship, SV will increase from a control equilibrium value (open circle) to a new equilibrium value (closed circle). Similarly, if the arterial resistance is increased, only the slope of the P_s-SV relationship will increase (thick arrow, Fig. 11*C*) without change in the ventricular P_s-SV relationship. Therefore, the SV under this condition will decrease from control value (open circle) to a new equilibrium (closed circle).

Potential sources of error in the coupling model. There appear to be two major sources of error in the proposed coupling model. One is the approximation of the end-systolic pressure by the end-ejection pressure. The other is the error associated with the approximation of the area under arterial pressure curve during systole. We have previously defined the end-systolic pressure as the pressure at which the time-varying ventricular volume elastance becomes maximum (10, 12), whereas the end-ejection pressure is defined as the pressure at which ventricular ejection is completed. These two pressures are not necessarily the same. However, it has been shown that under physiological or quasi-physiological loading conditions, these two pressures are in fact very close (8, 9). Therefore, the quantitative contribution of the difference to the stroke volume estimation seems insignificant.

In the estimation of A_s, two types of errors are potentially involved. One is the error resulting from the assumption of constant ejection time t_s regardless of the loading conditions. Since the ejection time can vary with changes in loading conditions, this variability could affect the accuracy of the estimation. The other is the error associated with the approximation of A_s by a rectangular area. The accuracy of this approximation certainly depends on the contour of arterial pressure curve during systole. Since changes in loading conditions can vary the contour of arterial pressure curve, even though most of the area under the systolic arterial pressure curve would

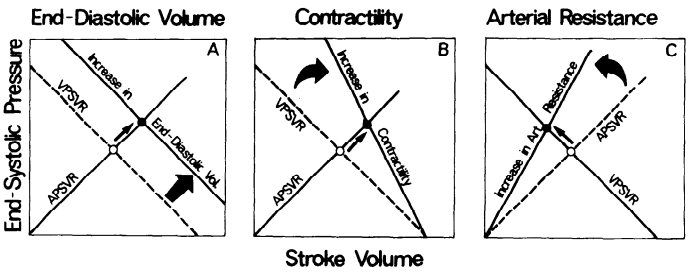

FIG. 11. *A*: effects of changes in end-diastolic volume on equilibrium stroke volume (SV). Ventricular P_s-SV relationship line (VPSVR) will shift rightward (*thick arrow*) with increases in end-diastolic volume. Arterial P_s-SV relationship line (APSVR) will not change with changes in ventricular preload. Equilibrium stroke volume will increase (*thin arrow*) from control (*open circle*) to the new steady state (*closed circle*) with an increase in end-diastolic volume. *B*: effects of changes in contractility on equilibrium SV. Ventricular P_s-SV relationship line becomes steeper (*thick arrow*) with increases in contractility. Equilibrium SV will increase as indicated by the shift in intersections (*thin arrow*) from control (*open circle*) to the new steady state (*closed circle*). *C*: effects of increase in arterial resistance on SV. Arterial P_s-SV relationship line is steeper (*thick arrow*) with increases in arterial resistance, while the ventricular P_s-SV is unchanged. Equilibrium SV decreases as shown by the shift in intersections (*thin arrow*) from control (*open circle*) to the new steady state (*closed circle*).

be represented by the rectangle, the accuracy of A_s estimation is, to some extent, loading-condition dependent. However, under physiological heart rate and contractility, the contribution of these errors in A_s estimation to the total area estimation (*Eq. 7*) may be attenuated because A_s is usually a minor fraction of the total area (A_T). Therefore, the minute variation of the ejection time and that of contour of arterial pressure curve associated with changes in the loading condition did not appear to influence substantially the accuracy of the stroke volume prediction. This indicates that the proposed coupling model could have a relatively large error in estimating stroke volume when the A_s becomes a large fraction of A_T (e.g., at high heart rates).

Another possible source of error is sensitivity of the ESPVR to loading conditions. Although some minor dependence of the ESPVR on loading conditions has been shown (9), the resultant error on SV estimation will be reasonably small from a quantitative point of view.

Afterload system. In this analysis, we used the three-element Windkessel model (19) as an approximation of the arterial system. Despite the simplicity of the model, its input impedance is reasonably similar to that of the natural arterial tree. The similarity is better in the low-frequency range than in the high-frequency range. Since most of the oscillatory power of arterial flow and pressure reside in the first several harmonics, the similarity of the impedance spectrum in the low-frequency range is more crucial than that in the high-frequency range. For the graphical coupling of the ventricular contractile function with the arterial load system using the P_s-SV relationship, a specific arterial model is not needed. However, for an analytic or quasi-analytic expression of the arterial P_s-SV relationship, a model is needed. Thanks to the simplicity of the three-element Windkessel model, we could derive an analytical equation (*Eq. 7*) to express SV

for a given set of the ventricular and arterial system parameters. The equation clearly illustrates how the lumped arterial system parameters (i.e., resistance and compliance) affect stroke volume. Such a global view is quite helpful in understanding the major mechanisms that determine the stroke volume through the ventriculoarterial interaction.

Limitations. The framework proposed was tested in isolated, blood-perfused canine left ventricles ejecting into a simulated arterial impedance. We maintained coronary arterial pressure constant throughout the experiments regardless of the ventricular loading conditions. In the real ventriculoarterial-coupled system, coronary arterial pressure is determined as the result of hydraulic interactions of the ventricle with the arterial impedance. Because coronary arterial pressure can modulate the ESPVR, particularly when it is low (15), stroke volume resulting in the natural circulatory system will be determined by a somewhat more complex mechanism than analyzed here. Therefore the proposed framework is valid only when the ventricle is operating, as it normally does, in a range of arterial pressures over which the ESPVR is relatively insensitive to changes in coronary perfusion pressure.

We are grateful to Kenneth Rent for excellent technical assistance.

This study was supported by National Heart, Lung, and Blood Institute Grants HL-14903 and Ischemic Heart Disease (SCOR) HL-17655.

Received 25 October 1982; accepted in final form 6 June 1983.

REFERENCES

1. GUYTON, A. C., AND A. W. LINDSEY. Circulatory filling pressure a determinant of cardiac output (Abstract). *Federation Proc.* 13: 63, 1954.
2. GUYTON, A. C. Determination of cardiac output by equating venous return curves with cardiac response curve. *Physiol. Rev.* 35: 123–129, 1955.
3. HERNDON, C. W., AND K. SAGAWA. Combined effects of aortic and right atrial pressures on aortic flow. *Am. J. Physiol.* 201: 102–108, 1969.
4. KAUFMANN, B. N., A. W. LINDSEY, AND A. C. GUYTON. Relationship of the mean circulatory filling pressure, right atrial pressure and venous return in dead dogs (Abstract). *Am. J. Physiol.* 179: 650, 1954.
5. PIENE, H. Interaction between the right heart ventricle and its arterial load: a quantitative solution. *Am. J. Physiol.* 238 (*Heart Circ. Physiol.* 7): H932–H937, 1980.
6. PIENE, H., AND T. SUND. Calculation of flow and pressure curves from the ventricular pressure-volume-time relationship and load impedance. In: *Cardiovascular System Dynamics: Models and Measurements*, edited by T. Kenner, R. Busse, and H. Hinghofer-Salkay. New York: Plenum, 1982, p. 47–56.
7. SAGAWA, K. The end-systolic pressure-volume relation of the ventricle: definition, modifications and clinical use. *Circulation* 63: 1223–1227, 1981.
8. SUGA, H. End-systolic pressure-volume relations (letter to the editor). *Circulation* 59: 419–420, 1979.
9. SUGA, H., A. KITABATAKE, AND K. SAGAWA. End-systolic pressure determines stroke volume from fixed end-diastolic volume in the isolated canine left ventricle under a constant contractile state. *Circ. Res.* 44: 238–249, 1979.
10. SUGA, H., AND K. SAGAWA. Instantaneous pressure-volume relationships and their ratio in the excised, supported canine left ventricle. *Circ. Res.* 35: 117–125, 1974.
11. SUGA, H., AND K. SAGAWA. End-diastolic and end-systolic ventricular volume clamper for isolated canine heart. *Am. J. Physiol.* 233 (*Heart Circ. Physiol.* 2): H718–H722, 1977.
12. SUGA, H., K. SAGAWA, AND A. A. SHOUKAS. Load independence of the instantaneous pressure-volume ratio of the canine left ventricle and effects of epinephrine and heart rate on the ratio. *Circ. Res.* 32: 314–332, 1973.
13. SUNAGAWA, K., D. BURKHOFF, K. LIM, AND K. SAGAWA. Impedance loading servo pump system for excised canine ventricle. *Am. J. Physiol.* 243 (*Heart Circ. Physiol.* 12): H346–H350, 1982.
14. SUNAGAWA, K., K. LIM, D. BURKHOFF, AND K. SAGAWA. Microprocessor control of a ventricular pump. *Ann. Biomed. Eng.* 10: 145–159, 1982.
15. SUNAGAWA, K., W. L. MAUGHAN, G. FRIESINGER, P. GUZMAN, M. CHANG, AND K. SAGAWA. Effect of coronary arterial pressure on left ventricular end-systolic pressure-volume relationship. *Circ. Res.* 50: 727–734, 1982.
16. TAYLOR, R., J. W. COVELL, AND J. ROSS, JR. Volume-tension diagrams of ejecting and isovolumic contractions in left ventricle. *Am. J. Physiol.* 216: 1097–1102, 1969.
17. WEBER, K. T., J. S. JANICKI, AND L. L. HEFNER. Left ventricular force-length relations of isovolumic and ejecting contractions. *Am. J. Physiol.* 231: 337–343, 1976.
18. WEBER, K. T., J. S. JANICKI, R. C. REEVES, L. D. HEFNER, AND T. J. REEVES. Determinants of stroke volume in the isolated canine heart. *J. Appl. Physiol.* 37: 742–747, 1974.
19. WESTERHOF, N., G. ELZINGA, AND P. SIPKEMA. Artificial arterial system for pumping hearts. *J. Appl. Physiol.* 31: 776–781, 1971.